Front. Optoelectron. 2013, 6(1): 108–113
DOI 10.1007/s12200-012-0296-4

RESEARCH ARTICLE

Structure and microwave properties analysis of substrate removed GaAs/AlGaAs electro-optic modulator structure by finite element method

Kambiz ABEDI (✉), Habib VAHIDI

Department of Electrical Engineering, Faculty of Electrical and Computer Engineering, Shahid Beheshti University, Tehran 1983963113, Iran

Abstract In this paper, structure and microwave properties of a substrate removed GaAs/AlGaAs traveling wave electro-optic modulator structure were analyzed and simulated by using the finite element numerical technique for lower loss, simultaneous matching of optical and microwave velocities and impedance matching with 50 Ω. The effects of core layer thickness, claddings thicknesses, and width of the modulator on the microwave effective index n_m were investigated, the characteristic impedance Z_C, the microwave losses α, and the half-wave voltage-length product $V_\pi L$ were calculated. The results of the simulation suggest that the electrical bandwidth of 22 GHz and the optical bandwidth of 48 GHz can be obtained for fully matched, lower loss structure, which correspond to a 13 V·cm drive voltage.

Keywords electro-optic modulators, finite element method (FEM), integrated optics, optical communication equipment

1 Introduction

The major requirement for ultra high speed optical communications is ultra wide band, low cost and low voltage modulators. These modulators can be categorized mainly in two groups of electro-optic and electro-absorption modulators. Different types of electro-optic modulators have been developed, including $LiNbO_3$ electro-optic modulators [1–3], semiconductor GaAs electro-optic modulators [4–6] and polymer electro-optic modulators [7]. Among these types of electro-optic modulators, polymer-based electro-optic modulators have more enhanced electro-optic coefficient than those of $LiNbO_3$ and GaAs semiconductor ones. However, most of the polymer electro-optic materials suffer from low thermal stabilities, and high initial electro-optic coefficients of polymer materials reduce with the time [7]. This thermal instability does not exist in $LiNbO_3$ electro-optic modulators. Also, large electro-optic coefficient of this electro-optic modulator is lower than that polymers one, but it is still much larger than that of semiconductors one. As a result, significant progress has been made for this type of modulators, and they are commercially available now. Nevertheless, these devices based on $LiNbO_3$ cannot be incorporated with semiconductor integrated devices. Therefore, they are only appropriate for external modulation applications [4]. However, compound semiconductors are suitable for such integration and have high refractive index and small dispersion of dielectric constant over a wide frequency band, up to optical frequencies. Due to these important advantages of $LiNbO_3$ electro-optic modulators, many efforts are made to design their structures with good capabilities, despite their very small electro-optic coefficients.

Two important parameters of optical modulators are bandwidth and drive voltage. Bandwidth of modulators is limited by the mismatch between microwave and optical wave speeds and the mismatch between characteristic impedance and source/load impedances (usually are 50 Ω). The drive voltage is dependent on electro-optic coefficient and interaction strength of microwave and optical wave. In addition, microwave attenuation has negative effect on modulator bandwidth. Lowering the microwave attenuation causes the decreasing of interaction between microwave and optical wave, which in turn increases modulator voltage [6]. Velocity matching in the case of semiconductor modulators can be obtained by using slow-wave electrodes that are capacitively loaded. Velocity matching design allows well electric field and optical mode

Received October 26, 2012; accepted November 20, 2012

E-mail: K_Abedi@sbu.ac.ir

overlapping. The possibility of this high overlapping combined with high refractive index is more than that of $LiNbO_3$ modulator, which results in low drive voltage devices even with bulk GaAs. The bulk GaAs substrate removed electro-optics modulators are one type of semiconductor modulators, which are constructed separately and then glued to semiconductor substrates. This technique allows placing contacts in both sides of epitaxially grown layers, which provide required loading without increasing microwave losses. This technique also allows the fabrication of ideal push-pull modulators and keeps the drive voltage low [8–10].

In this paper, structure and microwave properties of a substrate removed GaAs/AlGaAs traveling wave electro-optic modulator structure is analyzed and simulated using the finite element method (FEM) for lower loss, velocity matching and impedance matching with 50 Ω.

2 Modulator structure

The cross section of a substrate removed GaAs/AlGaAs traveling wave electro-optic modulator structure is shown in Fig. 1. This structure of electro-optic modulator is a single-arm Mach-Zehnder (MZ) modulator with modulator length l. The core material is GaAs. Ninety percent of AlGaAs material is chosen for constructing cladding layers. The ease of its growth on GaAs and its lower refractive index than that of GaAs provide good optical confinement. The refractive index is 3.377 for GaAs and 2.95 for $Al_{0.9}Ga_{0.1}As$. Two gold electrodes have been placed in both sides of these epitaxially grown layers. As we have mentioned above, the refractive index of GaAs in optical frequencies is about 3.377 and its relative permittivity in microwave frequencies is 13.18. For speed matching between two waves, the microwave speed needs to be slowed down.

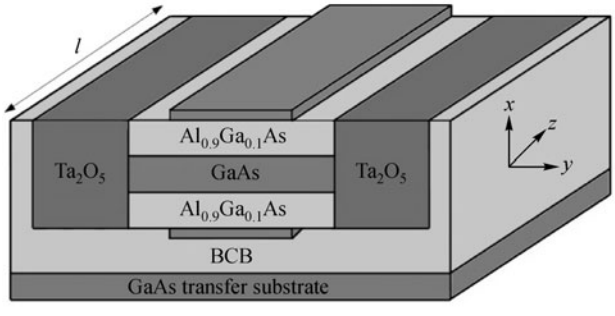

Fig. 1 Cross section of substrate removed GaAs/AlGaAs travelling wave electro-optic modulator

We need a new technique that could apply good loading to electrodes, and therefore materials that have high dielectric constant in microwave frequencies are required, but they do not deteriorate the optical confinement in optical frequencies. For this purpose Ta_2O_5 is chosen due to its unique properties with large dielectric constant (about 27) over microwave frequencies and low refractive index (about 2) in optical frequencies, which is helpful for good optical confinement [5]. The Ta_2O_5 are constructed in sides of main layers by using vapor deposition techniques. The width of these layers should be as the minimum as possible in order to provide the maximum loading. All of main layers and sidewall Ta_2O_5 layers are glued onto a transfer substrate using a benzo-cyclo-butane (BCB) polymer as a dielectric material with slight optical loss. The refractive index and relative permittivity of BCB are about 1.6 and 2.63, respectively.

3 Theory

Analysis of electro-optic modulators using the FEM is generally undertaken in two microwave and optical analysis phases [7]. In the microwave analysis, it is essential to determine the microwave effective index, n_m, characteristic impedance, Z_C, and microwave loss, α. Besides these characteristics in the microwave analysis, we determine static electric field that its effects on optical properties of materials like the optical effective index will be considered in optical analysis. In the other analysis, that is the optical analysis, some parameters, such as optical effective index, n_{eff}, and half-wave voltage length product, $V_\pi L$, can be determined.

The microwave effective index, n_m and microwave characteristic impedance, Z_C, which are related to capacitance of transmission line, can be determined as follows [11]:

$$n_m = \sqrt{C/C_0},$$

$$Z_C = \frac{1}{c\sqrt{CC_0}}, \tag{1}$$

where C is the capacitance per unit length of the transmission line, C_0 is the free space capacitance per unit length of the electrodes and c is the speed of light in the vacuum.

The other analysis is the optical analysis. For some reasons mentioned in Ref. [4], we consider quasi-transverse electric (TE) in optical analysis in this paper and take E_y component of electric field as the modulating electric field in this case. The quasi-TE analysis is based on the following summarization of the wave equation [11]:

$$\frac{n_x^2}{n_y^2}\frac{\partial^2 E_x}{\partial x^2} + \frac{\partial^2 E_x}{\partial y^2} - \beta^2 E_x + k_0^2 n_x^2 E_x = 0. \tag{2}$$

By obtaining β, optical effective index can be determined using $n_{eff} = \beta/k_0$, where k_0 is free space wave

number. By another optical analysis with the changing of

$$\Delta n_{xx} = -\Delta n_{zz} = \frac{n^3(x,y)}{2} r_{41} E_y(x,y)$$

in refractive index of core and cladding materials, we obtain another β that from these β values, and we can evaluate half wave length product voltage, $V_\pi L$, from Refs. [4,12].

$$V_\pi L = \frac{\pi V_0}{\Delta\beta},\ \Delta\beta = \beta_1 - \beta_0, \tag{3}$$

where V_0 is the applied voltage, β_1 and β_0 are the propagation constants of the fundamental E_x optical modes of MZ arms with and without the applied voltage, respectively. The value of r_{41} for GaAs has been taken equal to 1.6 pm/V. $V_\pi L$ is an important parameter in design of MZ interferometers that is defined as voltage per unit length needed to produce 180° phase difference in two arms. The optical wavelength is considered 1.55 μm in the optical analysis all over this paper.

Another key parameter that affects modulator bandwidth is the frequency dependent microwave loss, α, which can be expressed as the sum of dielectric loss, α_d, and conductor loss, α_c. These attenuations can be obtained from previously done microwave quasi-TE and magnetic analysis using below relations [13]:

$$\alpha_d(f) = \frac{p_d}{2p_o},\ \alpha_c(f) = \frac{p_c}{2p_o}, \tag{4}$$

where p_o is the time-averaged power flow along the line, and p_d and p_c are the time-averaged powers dissipated in the dielectrics and conductors, respectively. The way of computing these powers by the quasi-TEM is illustrated in Ref. [13].

Once all of these important parameters are acquired, modulator response in the most general form can be found from Ref. [11].

$$m(f) = \left| \frac{1 - S_1 S_2}{(1 + S_2)(e^{2ju_+} - S_1 S_2 e^{-2ju_-})} \times \left(e^{ju_+} \frac{\sin u_+}{u_+} + S_2 e^{-ju_-} \frac{\sin u_-}{u_-} \right) \right|, \tag{5}$$

where

$$S_1 = \frac{Z_1 - Z_C}{Z_1 + Z_C},\ S_2 = \frac{Z_2 - Z_C}{Z_2 + Z_C},$$

and

$$u_\pm = \frac{1}{c} f l (n_m \mp n_{eff}) - j\frac{1}{2}\alpha, \tag{6}$$

where, Z_1 and Z_2 are impedances of source and load, which are connected to the traveling wave modulator. And they are considered as 50 Ω, Z_C and n_m are the characteristic impedance and microwave effective index of the modulator, respectively, n_{eff} is the optical effective index, α is the microwave loss, c is the speed of light in vacuum, l is the modulator length, and f is the microwave frequency.

It should be noted that for precise calculation of this response, the frequency dependencies of all parameters are necessary to be considered. In quasi-TEM, we only consider frequency dependency for attenuations whereas microwave effective index, n_m, and characteristic impedance, Z_C, are also frequency dependent. For taking into account these frequency dependencies, it is necessary to do a full wave analysis.

Because of finite conductivity of gold electrodes and loss tangents of dielectrics, the eigen value will be complex in general in the form of $\gamma = \beta - j\alpha$. Therefore, the microwave effective index can be obtained from $n_m = \mathrm{Re}(\gamma)/k_0$ and the attenuation constant in Neper per meter can be derived from $\alpha = \alpha_c + \alpha_d = \mathrm{Im}(\gamma)$.

Also, the characteristic impedance of the line in this case, can be evaluated using the power current definition in the form of

$$Z_C = \frac{2P}{|I|^2}, \tag{7}$$

where P is modal power and I is the total current in z-direction carried by center electrode, and P and I in our FEM formulations can be evaluated by [3]

$$P = \frac{1}{2} \iint (E \times H^*) i_z \mathrm{d}x\mathrm{d}y,$$

and

$$I = \iint \sigma E_z \mathrm{d}x\mathrm{d}y, \tag{8}$$

where E and H are the electric and magnetic field vectors. The integration is done over the entire waveguide cross section for P and over the center electrode for I. σ is the electrode conductivity, i_z is the unit vector in the z-direction and * denotes the complex conjugate.

4 Results and discussion

In this section, a design over various physical characteristics of a substrate removed GaAs/AlGaAs traveling wave electro-optic modulator was carried out. Mainly, physical dimensions of layers were investigated to attain better performances. These dimensions include core layer thickness, thicknesses of claddings, and width of the modulator. Firstly, we investigated the effect of core region thickness on the microwave and optical characteristics. Figures 2(a) and 2(b) show the results of these effects. In Fig. 2(a), it is evident that when the core thickness increases, both Z_C and n_m increase, too. The proof of an increase in Z_C is that when core thickness increases,

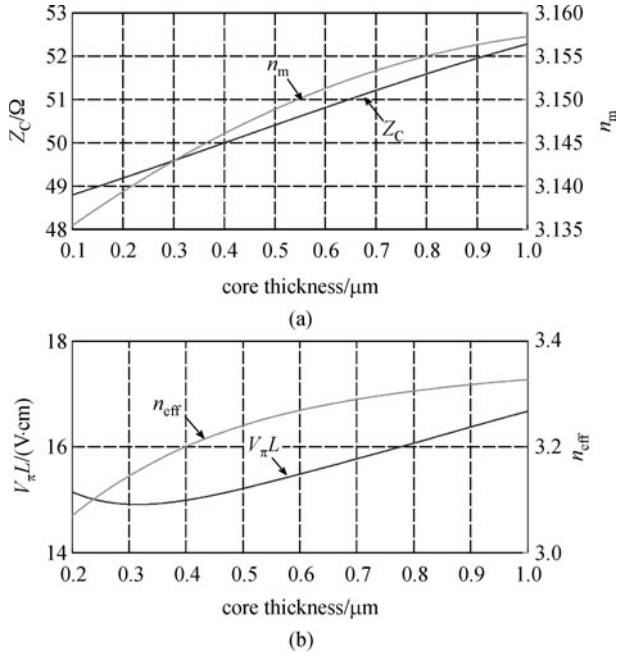

Fig. 2 Effects of increasing core thickness on (a) Z_C and n_m; (b) $V_\pi L$ and n_{eff}

capacitances of line (C and C_0) decrease and then from Eq. (1) characteristic impedance, Z_C, of line increases. Also with enlarging core thickness, the proportion of core thickness to cladding thickness increases and because the relative permittivity of core (≈ 13.18) is larger than that of claddings (≈ 10.372), resulting in total growth in effective permittivity of layers and thus the growth of n_m.

The variation of parameters vs. claddings thicknesses are shown in Figs. 3(a) and 3(b). The proof for these variations is similar to that for the core. Note that both down and top claddings change simultaneously.

The changing of Z_C in other figures can be proved in a similar way of the changing of line capacitance. However, the increase of Z_C with modulator width in Fig. 4(a) may be confused. In this case, we must note that the permittivity of core and layers are very lower than the permittivity of Ta_2O_5 and the modulator is surrounded by this high permittivity material rather than the vacuum.

This variation can be understood directly from the definitions of Z_C and n_m (Eq. (1)).

The variation of $V_\pi L$ can be understood from the variation of electric field intensity, which affects the refractive indexes of electro-optic materials in core and claddings. Then, with the increasing of the core and claddings thickness, the modulating electric field decreases and thus variation of propagation constant, β, with and without electric field declines, we will observe an enlargement in $V_\pi L$ (Figs. 2(b) and 3(b)). Figure 4(b) shows changes of $V_\pi L$ such as the very slow decreasing with broadening modulator width and then fast increasing. The results can be explained that with the increasing of modulator width up to electrode width, the modulating electric field inside electro-optic materials has almost no change firstly, but the optical effective index, n_{eff}, increases

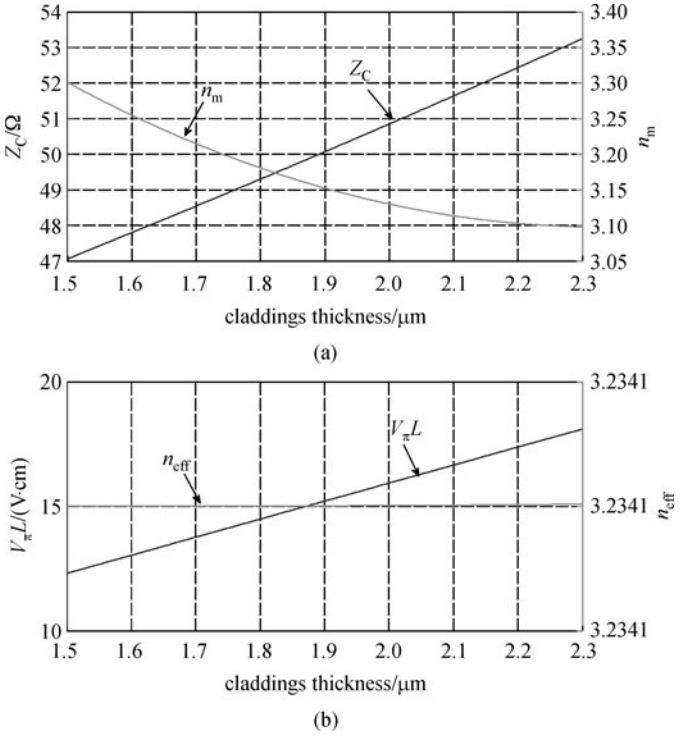

Fig. 3 Effects of increasing claddings thicknesses on (a) Z_C and n_m; (b) $V_\pi L$ and n_{eff}

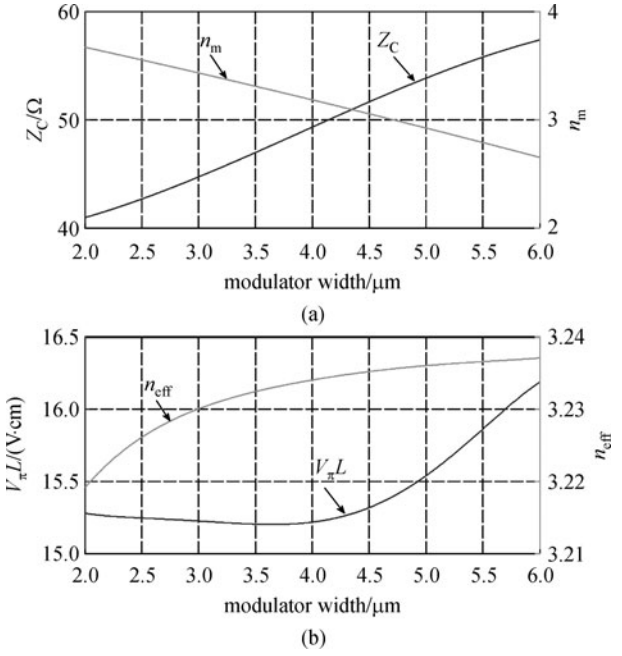

Fig. 4 Effects of increasing modulator width on (a) Z_C and n_m; (b) $V_\pi L$ and n_{eff}

contributing to the Δn, thus $\Delta\beta$ raises. As the modulator width is larger than the electrode width, the effective modulating electric field decreases rapidly resulting in increasing $V_\pi L$. Also, the way of changing n_{eff} can be understood from the relation, $n_{eff} = \beta/k_0$. For example, with increasing core thickness, large proportion of optical mode will be confined in core region that has large optical index compared to claddings and Ta_2O_5 side layers (Fig. 2(b)). The optical effective index, n_{eff}, does not depend on claddings thickness (Fig. 3(b)), because their thicknesses are always large enough to confine optical field in edges of themselves and no optical field could exit from the other side of claddings. Rising n_{eff} with increasing width of the modulator in Fig. 4(b) is because of good confinement of the optical mode in core region with enlarging modulator width that has larger refractive index compared to its neighbors.

The effects of modulator dimensions on microwave loss are important considerations that have been shown in Fig. 5. The frequency of this computation is 10 GHz. The microwave losses have very large effects on modulator response. The most important thing that could be understood from these figures is that any way causes the loss reduction, causes the $V_\pi L$ increment. That is why we cannot construct large bandwidth semiconductor modulators with acceptable low voltage. The only way to do this is the use of larger electro-optic coefficient materials to keep $V_\pi L$ low and then manipulating dimensions to decrease microwave loss.

In the design of modulator, two restrictions mainly affect the selection of modulator dimensions. One restriction is

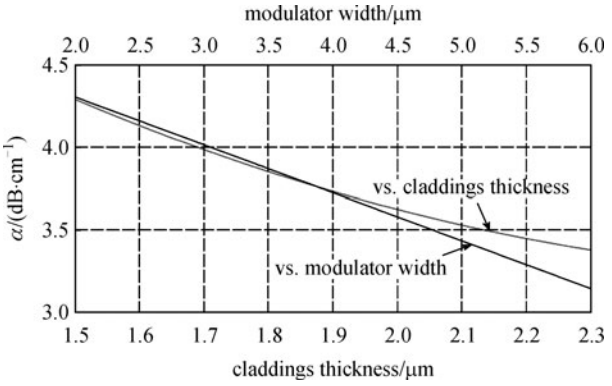

Fig. 5 Microwave loss α vs. cladding thickness and modulator width

associated with single mode operation requisite and the other is the fabrication limitation. For the ease of fabrication, the width of modulator must be greater than 2 μm. Also for single mode operation, thickness of core region must be less than 0.8 μm in this case. Therefore, we must define the large bandwidth and low voltage modulator. Semiconductor electro-optic modulators have been designed with drive voltage of 11.3 V and electrical bandwidth of 15 GHz for one planar microstrip structure (PMS) [6]. These results are reasonable. If we need to lower drive voltage, we must lower the frequency, vice versa.

One selection of dimensions has brought in Table 1 to study frequency dispersions of its parameters.

By obtaining precise frequency dependent values of the modulator parameters, we can evaluate modulator response from Eq. (5). In Fig. 6, the electrical and optical responses of the modulator are calculated using the values of n_m, Z_C and α obtained from full wave analysis. It is found from this figure that electrical bandwidth of about 22 GHz is acquired for this choice of dimensions. The half wave-length product for this selection of dimensions is about 13 V·m, which is relatively lower compared to some other similar works [6].

Table 1 Dimensions of substrate removed travelling wave electro-optic modulator

dimension	value
core thickness/μm	0.5
up-cladding thickness/μm	1.9
down-cladding thickness/μm	1.9
electrode thicknesses/μm	2.0
modulator width/μm	4.0
electrode width/μm	4.0
sidewall Ta_2O_5 widths/μm	25
modulator length/cm	1

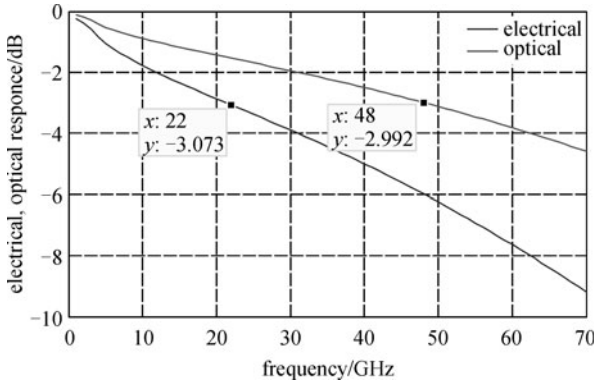

Fig. 6 Electrical and optical response of proposed modulator calculated from full-vectorial analysis

If we are interested in low voltage modulators, we can do another optimization and chose other dimensions to obtain lower bandwidth with lower $V_\pi L$. For example, It can be easily reached to low voltage modulators of $V_\pi L \approx 5\ \mathrm{V\cdot cm}$ in bandwidths of around 22 GHz. The corresponding optical bandwidth is 48 GHz for this electrical bandwidth.

Utilization of Ta_2O_5 in sides of modulator gives us a very good flexibility in changing values of n_m and Z_C in optimization procedure. If we would not use this material in sides of the modulator, in nearing n_m to n_{eff}, we would face with some limitation.

5 Conclusions

In this paper, a substrate removed GaAs/AlGaAs travelling wave electro-optic modulator was analyzed and simulated using the full vectorial finite element numerical technique for lower loss, simultaneous matching of optical and microwave velocities and impedance matching with 50 Ω. For this purpose, The effects of core layer thickness, claddings thicknesses, and width of the modulator on the microwave effective index n_m were investigated, and the characteristic impedance Z_C, the microwave losses α, and the half-wave voltage–length product $V_\pi L$ were calculated. The results of the simulation suggest that the electrical bandwidth of 22 GHz and the optical bandwidth of 48 GHz can be obtained for fully matched, lower loss structure, which correspond to a 13 V·cm drive voltage.

References

1. Rahman B M A, Haxha S. Optimization of microwave properties for ultrahigh-speed etched and unetched lithium niobate electrooptic modulators. IEEE Journal of Lightwave Technology, 2002, 20(10): 1856–1863
2. Gorman T, Haxha S. Thin layer design of X-cut lithium niobate electrooptic modulator with slotted SiO_2 substrate. IEEE Photonics Technology Letters, 2008, 20(2): 111–113
3. Gorman T, Haxha S. Design optimization of Z-cut lithium niobate electrooptic modulator with profiled metal electrodes and waveguides. IEEE Journal of Lightwave Technology, 2007, 25(12): 3722–3729
4. Obayya S S A, Haxha S, Rahman B M A, Grattan K T. Numerical modeling of polarization conversion in semiconductor electro-optic modulators. Applied Optics, 2005, 44(6): 1032–1038
5. Haxha S, Rahman B M A, Obayya S S A, Grattan K T. Velocity matching of a GaAs electro-optic modulator. Applied Optics, 2003, 42(36): 7179–7187
6. Cui Y S, Berini P. Modeling and design of GaAs traveling-wave electrooptic modulators based on the planar microstrip structure. IEEE Journal of Lightwave Technology, 2006, 24(6): 2368–2379
7. Gorman T, Haxha S, Ju J J. Ultra-high-speed deeply etched electrooptic polymer modulator with profiled cross section. IEEE Journal of Lightwave Technology, 2009, 27(1): 68–76
8. Shin J, Ozturk C, Sakamoto S R, Chiu Y J, Dagli N. Novel T-rail electrodes for substrate removed low-voltage high-speed GaAs/AlGaAs electrooptic modulators. IEEE Transactions on Microwave Theory and Techniques, 2005, 53(2): 636–643
9. Shin J, Wu S, Dagli N. 35-GHz bandwidth, 5-V-cm drive voltage bulk GaAs substrate removed electrooptic modulators. IEEE Photonics Technology Letters, 2007, 19(18): 1362–1364
10. Shin J, Wu S, Dagli N. Bulk undoped GaAs-AlGaAs substrate-removed electrooptic modulators with 3.7 V-cm drive voltage at 1.55 μm. IEEE Photonics Technology Letters, 2006, 18(21): 2251–2253
11. Koshiba M, Tsuji Y, Nishio M. Finite-element modeling of broadband traveling-wave optical modulators. IEEE Transactions on Microwave Theory and Techniques, 1999, 47(9): 1627–1633
12. Koshiba M, Maruyama S, Hirayama K. A vector finite element method with the high-order mixed-interpolation-type triangular elements for optical waveguide problems. IEEE Journal of Lightwave Technology, 1994, 12(3): 495–502
13. Pantic Z, Mittra R. Quasi-TEM analysis of microwave transmission lines by the finite-element method. IEEE Transactions on Microwave Theory and Techniques, 1986, 34(11): 1096–1103